Journal of Inflammation Research

Dovepress
Taylor & Francis Group

Open Access Full Text Article

ORIGINAL RESEARCH

Astragaloside IV Alleviates Osteoarthritis by Inhibiting Chondrocyte Ferroptosis via the p53/SLC7A11/GPX4 Axis

Zhongfu Tang[1,*], Lili Cheng[1,*], Ming Li[1], Junjie Chen[2], Chuanbing Huang[1]

[1]Department of Rheumatology, The First Affiliated Hospital of Anhui University of Chinese Medicine, Hefei, Anhui, 230031, People's Republic of China; [2]College of Traditional Chinese Medicine, Anhui University of Chinese Medicine, Hefei, Anhui, 230012, People's Republic of China

*These authors contributed equally to this work

Correspondence: Chuanbing Huang, Department of Rheumatology, The First Affiliated Hospital of Anhui University of Chinese Medicine, No. 117 Meishan Road, Shushan District, Hefei, Anhui, People's Republic of China, Email chuanbingh@ahtcm.edu.cn

Purpose: Osteoarthritis (OA) is a chronic joint disease characterized by articular cartilage damage. Astragaloside IV (AS-IV), a cyclic triterpenoid saponin extracted from Astragalus membranaceus, exhibits antioxidant and cartilage-protective activities. However, its mechanism of action in OA remains unclear. To study the efficacy and mechanism of action of AS-IV in the treatment of OA.

Methods: In the SW1353 cell model treated with IL-1β, cell viability was detected by CCK-8, and the ultrastructure of mitochondria was observed by transmission electron microscopy. Multiple methods such as flow cytometry, immunofluorescence, Western blotting, and fluorescent probe method were used to evaluate the effects of AS-IV on chondrocyte ferroptosis and extracellular matrix degradation, and the results were verified by rescue experiments. An OA rat model was established, and multiple methods such as histopathology were used to evaluate the therapeutic effect of AS-IV on OA cartilage injury.

Results: In vitro experiments have shown that IL-1β can induce ferroptosis in chondrocytes. Overexpression of p53 promotes ferroptosis in chondrocytes and exacerbates the progression of OA. AS-IV can downregulate the expression of p53 and MMP13, while upregulating the expression of SLC7A11, GPX4, SOX9, Col II, and GSH. Additionally, AS-IV reduces intracellular levels of ROS, MDA, and Fe^{2+}. In an OA rat model, AS-IV significantly reduces the Osteoarthritis Research Society International (OARSI) score and Mankin score, alleviating cartilage damage. Furthermore, AS-IV inhibits extracellular matrix degradation and lipid peroxidation in cartilage tissue.

Conclusion: AS-IV inhibits chondrocyte ferroptosis by modulating the p53/SLC7A11/GPX4 axis, thereby alleviating cartilage damage and OA. This suggests that AS-IV has therapeutic potential for OA treatment.

Keywords: osteoarthritis, astragaloside IV, chondrocytes, ferroptosis, lipid peroxidation

Introduction

Osteoarthritis (OA) is a common degenerative joint disease that affects the health and quality of life of a large number of people worldwide.[1] It is characterized by the progressive damage and destruction of articular cartilage, accompanied by pathological changes such as bone hyperplasia and synovitis.[2] Its clinical manifestations include joint pain, stiffness, and functional impairment.[3] With the intensification of population aging, the incidence of OA is increasing year by year. Obesity and joint injuries are risk factors for OA, and it is often complicated by other chronic diseases.[4] Currently, the treatment of OA mainly relies on non-steroidal anti- inflammatory drugs and intra-articular injection of corticosteroids to relieve symptoms, but these methods cannot cure the disease.[5] However, these drugs also carry risks of gastrointestinal toxicity and cardiovascular events. In recent years, more and more studies have been exploring whether the active ingredients of herbal medicines have the potential to treat OA.[6] Therefore, there is an urgent need to find new effective compounds to intervene in OA.

Received: 8 October 2025
Accepted: 14 November 2025
Published: 19 November 2025

Traditional Chinese medicine (TCM) has a long-standing history and abundant experience in treating OA.[7] Astragalus membranaceus, a well-known TCM herb used in China for millennia, possesses diverse pharmacological properties such as anti-inflammation, anti-oxidation, and osteoblast proliferation promotion.[8] In recent years, there has been growing interest in applying Astragalus membranaceus and its extracts to OA treatment.[9] AS-IV, a cyclic triterpenoid saponin from Astragalus membranaceus, has demonstrated notable anti-oxidative and cartilage-protecting activities.[10] Previous studies have revealed multiple beneficial effects of AS-IV. It can block CXCR4 signaling to prevent cartilage matrix degradation in OA rats.[11] It also promotes chondrocyte proliferation, inhibits apoptosis, and mitigates IL-1β-induced chondrocyte damage via autophagy inhibition.[12] Moreover, AS-IV reduces cell damage by activating the P62/Keap1/Nrf2 pathway to suppress ferroptosis.[13] Nevertheless, given that AS-IV acts on OA through multiple targets and pathways, its specific mechanism awaits further investigation.

The pathogenesis of OA is intricate, involving multiple interacting factors. Current consensus holds that inflammatory responses, oxidative stress, cell apoptosis, and extracellular matrix (ECM) degradation are pivotal in OA's onset and progression.[14] In recent years, ferroptosis, a novel form of programmed cell death triggered by iron-dependent lipid peroxidation, has drawn significant attention. It plays a crucial role in the apoptosis of OA chondrocytes.[15] Research indicates that chondrocyte ferroptosis is integral to OA pathogenesis, with the p53/SLC7A11/GPX4 axis being a key regulatory pathway.[16] p53, a well-known tumor suppressor gene, promotes ferroptosis when overexpressed.[17] Conversely, SLC7A11 and GPX4 are negative regulators of ferroptosis. Downregulation of SLC7A11 reduces intracellular glutathione (GSH) levels, increasing lipid peroxidation. GPX4, a glutathione peroxidase, catalyzes the reduction of lipid peroxides by GSH, safeguarding cells from ferroptosis.[18] p53 can inhibit the expression of SLC7A11, leading to GSH depletion and down - regulation of GPX4, causing extracellular matrix degradation and lipid peroxidation, and resulting in a ferroptosis state. As the core of ferroptosis regulation, an imbalance in the p53/SLC7A11/GPX4 signaling axis leads to the accumulation of intracellular reactive oxygen species (ROS) and accelerated ECM degradation.[19] However, it remains unclear whether AS-IV can regulate chondrocyte ferroptosis via this axis to intervene in OA.

Based on the aforementioned background, this study aims to investigate the efficacy and mechanism of AS-IV in treating OA. We hypothesize that AS-IV can inhibit chondrocyte ferroptosis by modulating the p53/SLC7A11/GPX4 signaling axis, thus alleviating articular cartilage damage in the OA model. Since human chondrosarcoma SW1353 cells have a clear response to inflammatory stimuli, they are suitable for simulating the OA microenvironment. IL-1β promotes ferroptosis of chondrocytes through multiple mechanisms, such as inducing oxidative stress, inhibiting the expression of GPX4, and increasing intracellular iron content. To test this hypothesis, we first established an in-vitro model of human chondrosarcoma SW1353 cells treated with IL-1β. We then employed multiple experimental methods to assess the effects of AS-IV on chondrocyte ferroptosis and ECM degradation. Subsequently, an in-vivo OA rat model was established using the monosodium iodoacetate (MIA) method to further validate the protective effect of AS-IV against cartilage damage. Through this research, we anticipate providing a theoretical basis for the application of AS-IV in OA treatment and laying the groundwork for developing more effective OA treatment strategies.

Materials and Methods

Cell Culture and IL-1β Stimulation

The human chondrosarcoma cell line SW1353 (SCSP-502, Cell Bank of the Chinese Academy of Sciences) was cultured in high-glucose DMEM (Gibco, Cat# 15140122) supplemented with 10% FBS (Gibco, Cat# 10270106) and 1% penicillin/streptomycin (Gibco, Cat# 15140122) at 37°C with 5% CO_2. Cells were passaged using 0.25% trypsin-EDTA (Gibco, Cat# 25200056) when they reached 80–90% confluence. Logarithmic phase cells were used for all experiments. To determine the optimal IL-1β concentration, SW1353 cells were stimulated with various concentrations of recombinant human IL-1β (PeproTech, Cat# 200–01B) for 24 hours.

Cell Viability Assay

The effects of different treatments on the viability of SW1353 cells were evaluated using the CCK-8 method. SW1353 cells were seeded in 96-well plates at a density of 1×10^4 cells per well, and 6 replicate samples were set for each condition. During the last 2 hours of the culture process, 10 μL of CCK-8 reagent (Dojindo, Cat# CK04) was added to each well, and the absorbance of each well was measured at OD 450 nm using an enzyme-linked immunosorbent assay reader.

Cell Transfection

After trypsinization and counting, seed SW1353 cells into a 6-well plate at a density of 3×10^5 cells per well in 2 mL of DMEM with 10% FBS. Incubate for 24 hours until 70% confluence is reached. For transfection: Prepare complexes by mixing 125 μL Opti-MEM (serum-free) with 2.5 μg plasmid DNA (pcDNA3.1-p53 for the experimental group, pcDNA3.1 empty vector for the control group). Aspirate the old medium from each well, add 1 mL of fresh complete medium, and then add the transfection complexes dropwise. Incubate at 37°C/5% CO_2 for further culture.

Animals and Modeling

Forty male Sprague-Dawley (SD) rats weighing 180 ± 20 g were sourced from Speford (Suzhou) Biotechnology Co., Ltd. (License No.: SCXK (Su) 2022–0006). The rats were housed in a controlled environment at 25 ± 2 °C, with a 12-hour light/dark cycle and 50% - 60% humidity, and provided with ad libitum food and water. After a 1 - week acclimation period, all experimental operations were conducted following the "Guide for the Care and Use of Laboratory Animals" and approved by the Experimental Animal Ethics Committee of the First Affiliated Hospital of Anhui University of Chinese Medicine (AZYFY-2025-1017). The osteoarthritis model was established using the MIA method.[20] For 4 weeks, 50 μL of a 30 mg/mL MIA solution (Sigma, Cat# I2512) was injected daily into the rats' knee-joint cavities. All procedures and operations of the experiment were strictly carried out in accordance with The ARRIVE guidelines 2.0 (https://arriveguidelines.org/).

Animal Experiment Grouping and Treatment

Forty SD rats were randomly divided into four groups: (1) Sham operation group (Sham, n = 10); (2) Osteoarthritis model group (MIA, n = 10); (3) Astragaloside IV group (AS - IV, 40 mg/kg/d, n = 10); (4) Celecoxib group (Celecoxib, 30 mg/kg/d, n = 10). Gastric gavage treatment was started one week after modeling. The sham operation group and the model group were given an equal volume of normal saline for 4 consecutive weeks. After 4 weeks of treatment, the rats were anesthetized with 5% isoflurane gas. Whole blood was collected and centrifuged to obtain serum samples, which were stored at −80°C. Subsequently, Euthanize rats with carbon dioxide according to the guidelines of the American Veterinary Medical Association (https://www.avma.org/). Knee joint cartilage tissues were collected for subsequent experiments.

Histopathology

The cartilage tissue was fixed in 4% paraformaldehyde (Sigma, Cat# P6148) for 48 h, then rinsed under running water. Dehydration was performed using ethanol, followed by clearing in xylene (Sigma, Cat# 214736). The tissue was embedded in paraffin, and then sectioning and dewaxing procedures were carried out. The sections were stained with hematoxylin-eosin[21] and Safranin O/Fast Green[22] respectively, and observed and recorded under an optical microscope. Meanwhile, the degree of cartilage injury was evaluated by Mankin score and OARSI score.[23]

Detection of ROS by Flow Cytometry

Place the cartilage tissue sections into PBS containing trypsin and digest them at 37°C for 30 min. Collect the cells, add DCFH-DA (Beyotime, Cat# S0033S) at a concentration of 10 μmol/L, and incubate at 37°C for 20 min. Load the cell suspension onto a flow cytometer (Beckman, CytoFLEX). Analyze the data using FlowJo_V10 software and calculate the fluorescence intensity of ROS-positive cells. Meanwhile, the steps for detecting intracellular ROS in SW1353 cells are as described above.

Determination of Fe^{2+}

For the determination of Fe^{2+} in SW1353 cells, the fluorescent probe method was used for detection. SW1353 cells were seeded in a 96-well black-bottom plate, and a staining buffer containing 2 μM fluorescent probe was added. The detection was carried out using a fluorescent probe kit (MCE, Cat# HY-D1055). For the determination of Fe^{2+} in cartilage tissue, the frozen section probe method was used for detection. Tissue sections were treated with 0.1% hyaluronidase for

20 min, incubated with the HY-D1057 working solution in the dark, the fluorescence intensity of the quantitative region was measured, and the proportion of Fe^{2+} in the tissue region was estimated.

Determination of MDA and GSH

For the determination of MDA and GSH in SW1353 cells, collect the cells, lyse them and centrifuge to obtain the supernatant. Then, use the MDA kit (Nanjing Jiancheng Bioengineering Institute, Cat# A003-1) and GSH kit (Nanjing Jiancheng Bioengineering Institute, Cat# A006-2-1) to detect the contents of MDA and GSH. For cartilage tissue, after homogenizing an appropriate amount of cartilage tissue, add TBA solution for reaction, centrifuge to obtain the supernatant and measure the absorbance. Calculate the concentrations of MDA and GSH in the samples according to the standard curve.

Transmission Electron Microscope (TEM)

The cartilage tissue was fixed in 2.5% glutaraldehyde (Sigma, G5882), and then fixed again in 1% osmium acid (Sigma, 208164). After dehydration with gradient ethanol, resin infiltration and embedding, ultrathin sections were prepared. The sections were stained with 2% uranyl acetate for 30 min and lead citrate for 5 min, and then thoroughly rinsed with distilled water to avoid stain crystallization. The structure of the cartilage tissue was observed and recorded using a transmission electron microscope. For SW1353 cells, the cells in the culture medium were collected, an appropriate amount of trypsin-EDTA digestive solution was added. After centrifuging the cell suspension, the cell pellet was collected, and the subsequent experimental steps were the same as above.

Real-Time Quantitative Polymerase Chain Reaction (RT-qPCR)

Collect the cell pellet, add 1 mL of TRIzol for lysis, perform layering and RNA precipitation to complete RNA extraction. Conduct the RT reaction to obtain cDNA. Use a PCR instrument to perform the RT-qPCR reaction for detection, and calculate the relative mRNA expression level using the $2^{-\Delta\Delta Ct}$ method. All experiments were repeated three times. The primer sequences are as follows: p53 (forward sequence: 5'-GTAGTTTCTACAGTTGGGCA-3' and reverse sequence: 5'-GATGG GGTGAGATTTCCTTT-3'), SLC7A11 (forward sequence: 5'-ACCTTTGAGTTTTCACCTGT-3' and reverse sequence: 5'-AACAGGCTTTCTGACCATAG-3'), GPX4 (forward sequence: 5'-CAGGAGCCAGGGAGTAAC-3' and reverse sequence: 5'-CCTTGGGTTGGATCTTCA-3'), β-actin (forward sequence: 5'-CCCTGGAGAAGAGCTACGAG-3' and reverse sequence: 5'-GGAAGGAAGGCTGGAAGAGT-3').

Molecular Docking

Download the molecular structures of p53, SLC7A11, and GPX4 from the PDB database (https://www.rcsb.org/), and download the three - dimensional structure of Astragaloside IV from the PubChem database (https://pubchem.ncbi.nlm.nih.gov/). Use the AutoDock Vina software for molecular docking to explore the possible binding sites. Visualize the docking results using the PyMOL software and evaluate the binding ability between the ligand and the receptor.

Western Blotting

Add 600 μL of RIPA cell lysis buffer to the cartilage tissue samples for lysis, collect the supernatant, or collect chondrocytes. Add 5X SDS-PAGE protein loading buffer. Place the cooled protein samples into the wells of the SDS-PAGE gel and perform protein electrophoresis for 1 h. Incubate with primary antibodies: Add SOX9 (Abmart, Cat# T55400, 1:1000), Col II (Bioss, Cat# bs-10589R, 1:1000), MMP13 (Abcam, Cat# ab39012, 1:3000), p53 (Proteintech, Cat# 60283-2-Ig, 1:5000), p-p53 (Proteintech, Cat# 80195-1-RR, 1:5000), SLC7A11 (Proteintech, Cat# 26864-1-AP, 1:4000), GPX4 (Abclonal, Cat# A1933, 1:50,000), and GAPDH (Zsbio, Cat# TA-08, 1:5000), then add the HRP-labeled secondary antibody (1:20000) and incubate at room temperature for 1.2 h. Use the ECL luminescence kit (Biosharp, Cat# BL520A) to take photos with a chemiluminescence imaging system and save them. Use Image J software for gray-scale analysis.

Immunofluorescence Staining

The cartilage tissue sections were placed in xylene (Sigma, Cat# 214736) for dewaxing, or the cell samples were fixed. Then, antigen retrieval was performed. 0.3% Triton X-100 (Ebiogo, Cat# B025) was added for permeabilization and blocking at room temperature. The primary antibodies were added drop-by-drop: MMP13 (Abcam, Cat# ab39012, 1:500), SLC7A11 (Abcam, Cat# ab307601, 1:500), SOX9 (Santa, Cat# sc-166505, 1:300), Col II (Santa, Cat# sc-52658, 1:300), GPX4 (Proteintech, Cat# 60283-2-Ig, 1:5000), and incubated at 37°C for 60 min. The secondary antibody: an appropriate amount of HRP-labeled secondary antibody reagent (Fuzhou Maixin, Cat# KIT5030) was added drop-by-drop. An appropriate amount of DAPI staining solution was added drop-by-drop to counterstain the sections. The sections were observed and images were collected under a fluorescence microscope (Olympus, BX43).

Immunohistochemical Staining

The cartilage tissue sections were placed in 3% H_2O_2 and incubated at room temperature for 10 min. Then, 5% BSA was added dropwise and sealed at room temperature for 30 min. The primary antibodies were added dropwise: p53 (Proteintech, Cat# 10442-1-AP, 1:500), GPX4 (Proteintech, Cat# 67763-1-Ig, 1:2000), SOX9 (Abcam, Cat# ab185966, 1:1000), Col II (Proteintech, 28459-1-AP, 1:2000), and incubated at 37°C for 60 min. The secondary antibody was added dropwise and incubated at 37°C for 30 min. Counterstaining with hematoxylin was performed for 2 min, and bluing in lithium carbonate solution for 30s. The sections were mounted with neutral gum, and the results were observed under a microscope (Olympus, CX41).

Statistical Analysis

The SPSS 25.0 software and GraphPad Prism 9.0 software were used for data statistical analysis and visualization. All data were from at least three repeated experiments, and each repeated experiment was independently detected three times. Measurement data were expressed as mean ± standard deviation. For the comparison between groups, the independent-sample *T*- test was used for data conforming to the normal distribution, and the non-parametric test was used for data not conforming to the normal distribution. A P value < 0.05 was considered statistically significant.

Results

IL-1β Induces Ferroptosis in Chondrocytes and Downregulates the Expression of SLC7A11 and GPX4

Chondrocyte ferroptosis is intricately linked to the severity of cartilage injury and plays a significant role in the pathogenesis of osteoarthritis.[24] To establish an in-vitro osteoarthritis cell model, SW1353 cells were treated with IL-1β.[25] First, we conducted a dose-response experiment. SW1353 cells were exposed to varying concentrations of IL-1β (0, 2.5, 5, 10, 20 ng/mL) for 24 hours, and cell viability was assessed. The results revealed that 10 ng/mL of IL-1β was the optimal concentration for stimulating SW1353 cells (Figure 1A). Immunofluorescence staining was employed to detect the expression of SLC7A11 and GPX4. Compared with the Control group, after IL-1β induction, the expression levels of SLC7A11 and GPX4 in chondrocytes were significantly reduced ($P < 0.001$, Figure 1B–D). Transmission electron microscopy was used to examine the mitochondrial ultrastructure of SW1353 cells in both groups. In the Control group, mitochondria exhibited an oval or long-rod shape, with distinct inner membrane cristae and continuous, intact outer membranes. In contrast, after IL-1β induction, mitochondria showed marked atrophy, with partial disintegration of the outer membrane, disappearance of the inner membrane cristae, and increased membrane density (Figure 1E). These mitochondrial alterations are characteristic features of ferroptosis in SW1353 cells, providing further evidence that IL-1β can induce chondrocyte ferroptosis. RT-qPCR analysis was also performed. Compared with the Control group, the mRNA expression of p53 in the IL-1β group was upregulated, while the mRNA expression of SLC7A11 and GPX4 was downregulated ($P < 0.01$, Figure 1F). Collectively, these findings suggest that IL-1β stimulation of SW1353 cells can trigger changes in the p53/SLC7A11/GPX4 ferroptosis pathway. This is the verification of the results that IL-1β can induce SW1353 cells to construct an OA ferroptosis model.

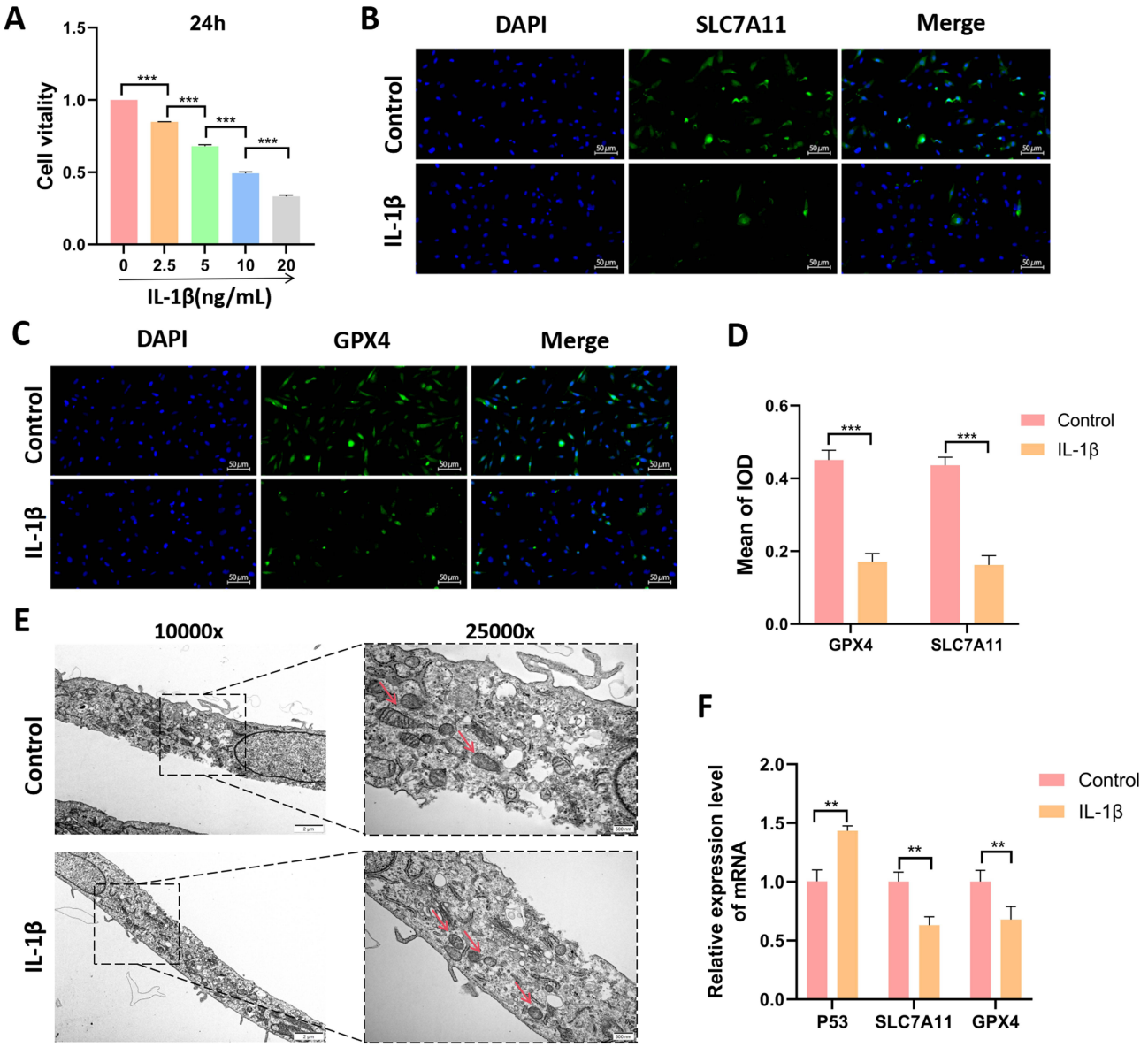

Figure 1 IL-1β induces ferroptosis in chondrocytes and downregulates the expression of SLC7A11 and GPX4. (**A**) Screening of the optimal concentration of IL-1β for inducing SW1353 cells. (**B** and **C**) Immunofluorescent staining of SLC7A11 and GPX4 (scale bar: 50 μm). (**D**) Comparison of average fluorescence intensity values (n = 3). (**E**) Transmission electron microscopy observation of the ultrastructure of chondrocyte mitochondria (scale bars: 2 μm and 500 nm). (**F**) RT-qPCR detection of the mRNA levels of p53, SLC7A11, and GPX4 (n = 10). **P < 0.01, ***P < 0.001. The red arrow indicates the mitochondrial morphology. All data are from at least three repeated experiments, and each repeated experiment was independently detected three times.

AS-IV Can Effectively Inhibit Matrix Degradation, Lipid Peroxidation, and Ferroptosis in IL-1β-Induced SW1353 Cells

To explore the effects of AS-IV on IL-1β-induced SW1353 cells, the CKK-8 method was first used to detect the cell viability under the intervention of different concentrations (0, 15, 25, 50, 70 μM) of AS-IV. The results showed that the optimal intervention concentration of AS-IV was 25 μM, and the intervention time was 24 h (Figure 2A). The cells were divided into four groups, in which Ferrostatin-1 (Fer-1), an inhibitor of ferroptosis, was used as the positive control group. The CKK-8 method was used to detect the cell viability (Figure 2B). The intracellular Fe^{2+} content was detected by the fluorescent probe method. After IL-1β induction, the Fe^{2+} content increased ($P < 0.001$). After the intervention of AS-IV and Fer-1, the intracellular Fe^{2+} content decreased ($P < 0.01$, Figure 2C). To evaluate the effect of AS-IV on the matrix degradation of SW1353 cells, Western blotting was used to detect the protein expression levels of SOX9, Col II,

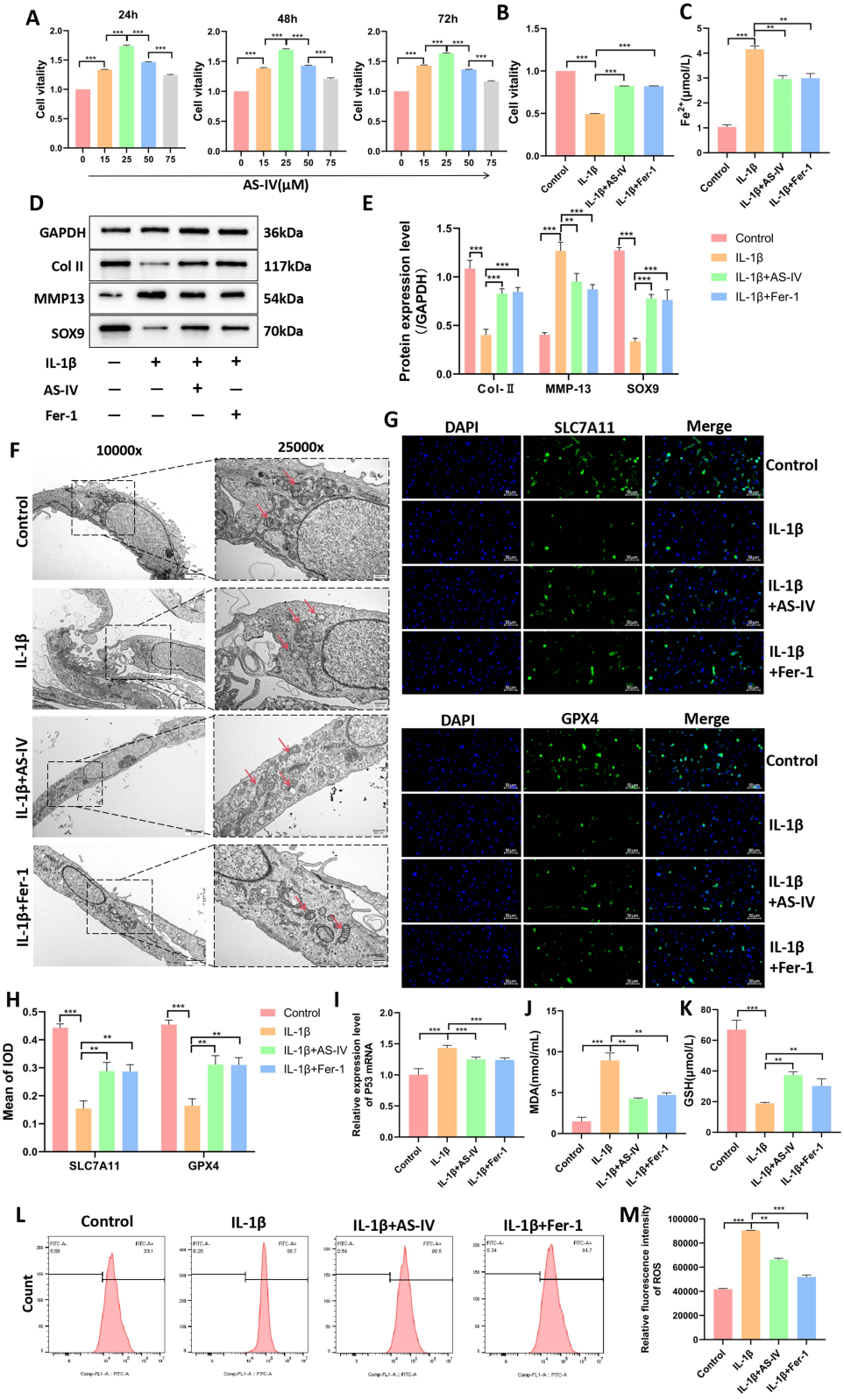

Figure 2 AS-IV can effectively inhibit matrix degradation, lipid peroxidation, and ferroptosis in IL-1β-induced SW1353 cells. (**A**) Screening of the optimal intervention concentration and time of AS-IV. (**B**) Determination of cell viability in each group. (**C**) Determination of Fe^{2+} content (n = 10). (**D** and **E**) Western blotting was used to detect the protein levels of SOX9, Col II, and MMP13 in each group of cells (n = 3). (**F**) Transmission electron microscopy was used to observe the changes in mitochondrial ultrastructure in each group of cells (scale bars: 2 μm and 500 nm). (**G** and **H**) Immunofluorescent staining was used to detect the expression of SLC7A11 and GPX4 (scale bar: 50 μm). (**I**) RT-qPCR was used to detect the expression level of p53 mRNA (n = 10). (**J** and **K**) Determination of MDA and GSH in each group of cells. (**L** and **M**) Flow cytometry was used to detect the intracellular ROS levels in each group of cells. **P < 0.01, ***P < 0.001. The red arrow indicates the mitochondrial morphology. All data were from at least three repeated experiments, and each repeated experiment was independently detected three times.

https://doi.org/10.2147/JIR.S572167

and MMP13 in the cells. The results showed that the expression levels of SOX9 and Col II in the IL-1β group were lower than those in the Control group, and the expression level of MMP13 was higher than that in the Control group ($P < 0.001$). After AS-IV intervention, the expression levels of SOX9 and Col II increased, and the expression level of MMP13 decreased ($P < 0.001$, Figure 2D and E), which was consistent with the effect of Fer-1 intervention. SOX9 is the core transcription factor regulating cartilage differentiation, Col II is the main component of the extracellular matrix of chondrocytes, and MMP13 can degrade cartilage matrix components such as Col II. AS-IV can upregulate the levels of SOX9 and Col II and downregulate the level of MMP13. These results indicate that AS-IV can inhibit the matrix degradation of SW1353 cells. Ferroptosis was evaluated by observing the ultrastructure of cell mitochondria through transmission electron microscopy. Compared with the IL-1β group, after AS-IV intervention, the mitochondrial volume was close to normal, the cristae structure was partially reconstructed, short tubular or lamellar cristae were visible, and the membrane density decreased (Figure 2F). This was comparable to the effect after Fer-1 intervention, indicating that AS-IV can inhibit ferroptosis. Then, RT-qPCR and immunofluorescence staining were used to detect the effect of AS-IV on the p53/SLC7A11/GPX4 pathway. The results showed that AS-IV could reduce the mRNA expression of p53 and increase the expression of SLC7A11 and GPX4 ($P < 0.01$, Figure 2G–I). Finally, the levels of GSH, MDA, and ROS were detected to evaluate lipid peroxidation. The intervention effects of AS-IV and Fer-1 were consistent, which could reduce the intracellular levels of MDA and ROS and increase the level of GSH ($P < 0.01$, Figure 2J–M). The above results fully demonstrate that AS-IV can effectively inhibit ferroptosis and lipid peroxidation in SW1353 cells.

Effects of p53 Overexpression on the p53/SLC7A11/GPX4 Axis, Lipid Peroxidation, and Ferroptosis

To investigate the effects of p53 overexpression on ferroptosis and lipid peroxidation, we transfected the pcDNA3.1-p53 plasmid into SW1353 cells to establish a p53 overexpression state. The results showed that compared with the pcDNA3.1-NC group, the levels of p-p53 protein and p53 mRNA in the pcDNA3.1-p53 group were increased, while the expression levels of SLC7A11 and GPX4 proteins and mRNAs were decreased ($P < 0.001$, Figure 3A–C). In the

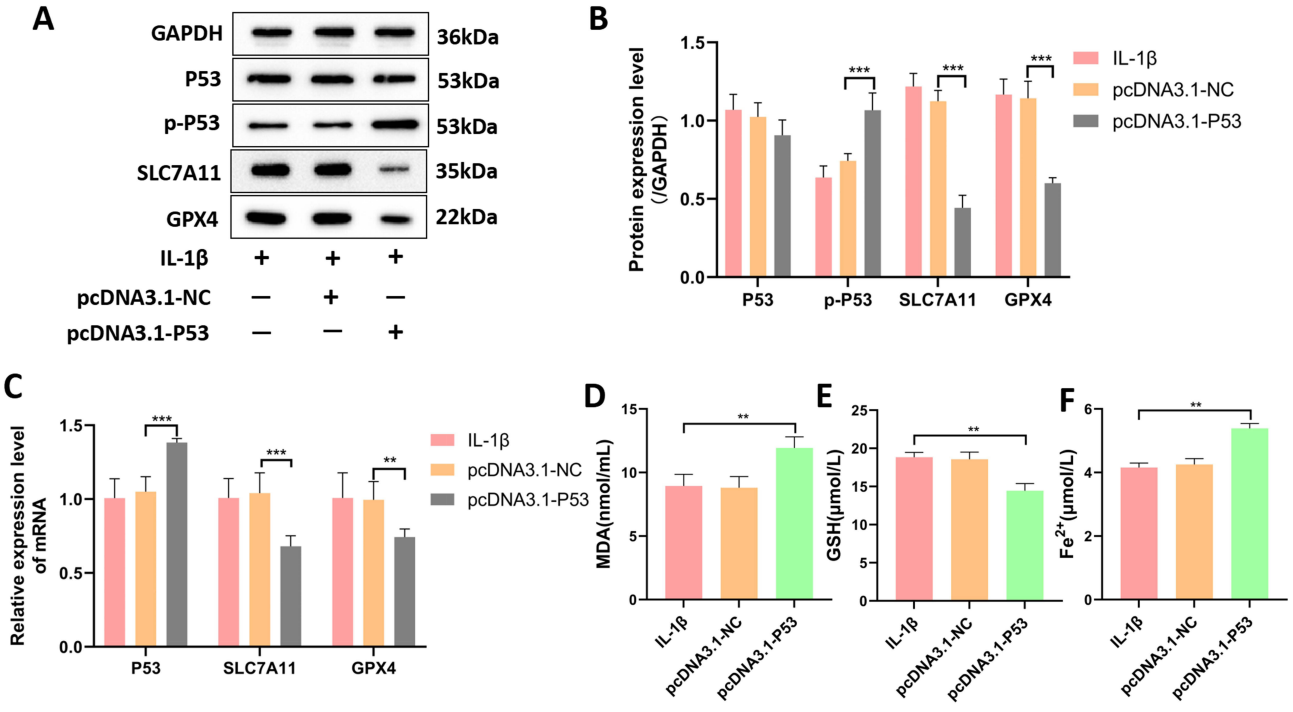

Figure 3 Effects of p53 overexpression on the p53/SLC7A11/GPX4 axis, lipid peroxidation, and ferroptosis. (**A** and **B**) Western blotting was used to detect the protein levels of p53, p-p53, SLC7A11, and GPX4 in each group of cells (n = 3). (**C**) RT-qPCR was used to detect the mRNA expression levels of p53, SLC7A11, and GPX4 (n = 10). (**D–F**) The contents of GSH, MDA, and Fe2+ in each group of cells were measured (n = 10). **P < 0.01, ***P < 0.001.

pcDNA3.1-p53 group, the level of MDA was increased, the level of GSH was decreased (P < 0.01, Figure 3D and E), and the content of Fe^{2+} was increased ($P < 0.01$, Figure 3F). These results fully indicate that p53 overexpression can exacerbate lipid peroxidation and ferroptosis in SW1353 cells.

Overexpression of p53 Can Reverse the Inhibitory Effect of AS-IV on Ferroptosis of Chondrocytes

To investigate whether the treatment with AS-IV affects chondrocyte ferroptosis by downregulating the expression of p53, we transfected the pcDNA3.1-p53 plasmid into SW1353 cells on the basis of AS-IV intervention. Western blotting was used to detect the protein levels of SLC7A11 and GPX4 in cells of each group. Compared with the IL-1β + AS-IV + pcDNA3.1-NC group, the protein levels of SLC7A11 and GPX4 in the IL-1β + AS-IV + pcDNA3.1-p53 group were increased ($P < 0.01$, Figure 4A–C). Compared with the IL-1β group, the mitochondrial volume in cells of the IL-1β + AS-IV group was close to normal, the cristae structure was partially reconstructed, short tubular or lamellar cristae were visible, and the membrane density was decreased. After overexpressing p53 on the basis of AS-IV treatment, the mitochondrial volume decreased, the cristae structure partially disappeared, and the membrane density increased (Figure 4D). Meanwhile, the intracellular Fe^{2}+ content increased after overexpressing p53 ($P < 0.01$, Figure 4H). These results indicate that overexpressing p53 can reverse the inhibitory effect of AS-IV on chondrocyte ferroptosis. The expression levels of Col II, SOX9, and MMP13 were detected to evaluate whether overexpressing p53 affects the inhibition of lipid peroxidation by AS-IV. Compared with the control group, the expression of Col II and SOX9 decreased and the expression of MMP13 increased after overexpressing p53 ($P < 0.01$, Figure 4E–G). RT-qPCR was used to detect the mRNA expression of the p53/SLC7A11/GPX4 axis. Compared with the control group, overexpressing p53 could increase the mRNA expression of p53 and decrease the mRNA expression of SLC7A11 and GPX4 ($P < 0.01$, Figure 4I–K). The above results indirectly indicate that AS-IV can inhibit chondrocyte ferroptosis by mediating the p53/SLC7A11/GPX4 axis.

AS-IV Can Improve Cartilage Damage and Inhibit Matrix Degradation in OA Rats

To further explore the potential efficacy of AS-IV against OA, a rat model of OA was established using the MIA method. The animals were divided into four groups: Sham group, MIA group, AS-IV group, and Celecoxib group. HE staining and Safranin O/Fast Green staining were performed on cartilage tissues to evaluate the protective effect of AS-IV on cartilage. Compared with the Sham group, the MIA group showed destruction of cartilage structure, disordered arrangement of chondrocytes, blurred tidemark, and severe loss of proteoglycans. Compared with the MIA group, the AS-IV group exhibited reduced surface roughness and defect degree of articular cartilage, partial restoration of the cellular hierarchical structure, alleviated abnormalities of the tidemark, and partial containment of proteoglycan loss (Figure 5A). This was consistent with the effect of Celecoxib treatment. Meanwhile, AS-IV improved the pathological changes of cartilage tissues by reducing the OARSI score and Mankin score ($P < 0.001$, Figure 5B and C). Regarding the degradation of the extracellular matrix, the expression of Col II, SOX9, and MMP13 was detected by immunohistochemistry and immunofluorescence staining. After AS-IV treatment, similar to the effect of Celecoxib intervention, the expression of Col II and SOX9 in cartilage tissues increased, while the expression of MMP13 decreased ($P < 0.01$, Figure 5D–G). In conclusion, AS-IV can inhibit the degradation of the extracellular matrix in OA rats and improve the degree of cartilage damage.

AS-IV Can Regulate the p53/SLC7A11/GPX4 Pathway in Cartilage Tissue

To verify the interaction between AS-IV and the p53/SLC7A11/GPX4 axis, molecular docking of AS-IV with p53, SLC7A11, and GPX4 was performed respectively. The binding energy of AS-IV with p53 was −6.6 kcal/mol, and it formed 2 hydrogen bonds with the ARG-37 residue; the binding energy of AS-IV with SLC7A11 was −9.2 kcal/mol, it formed 1 hydrogen bond with the ASN-382 residue and 2 hydrogen bonds with the SER-318 residue; the binding energy of AS-IV with GPX4 was −7.3 kcal/mol, and it formed 1 hydrogen bond with each of the SER-45, HIS-141, and ARG-32 residues (Figure 6A). Then, experimental verification was carried out through immunohistochemistry,

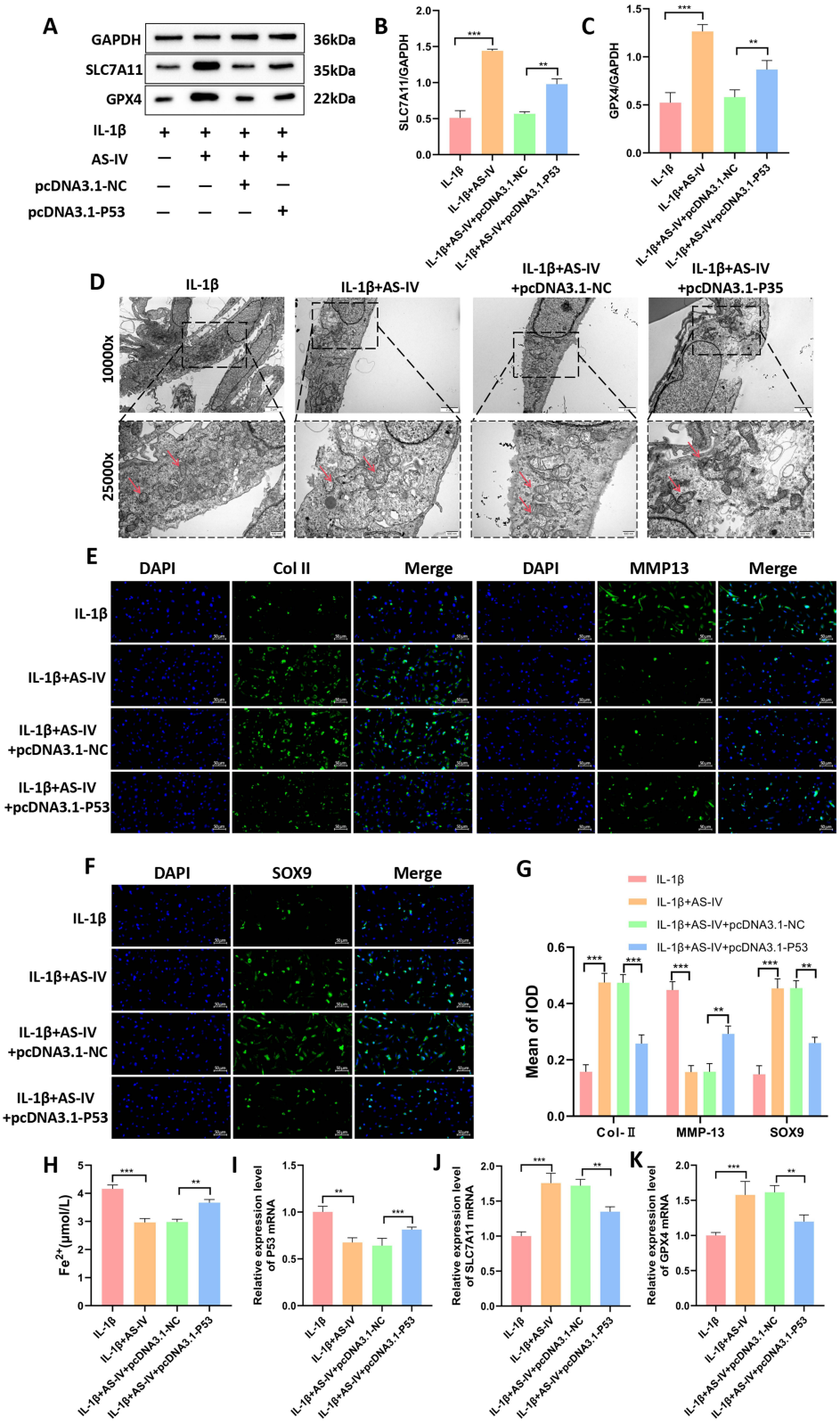

Figure 4 Overexpression of p53 can reverse the inhibitory effect of AS-IV on ferroptosis in chondrocytes. (**A**–**C**) Western blotting was used to detect the protein levels of SLC7A11 and GPX4 in each group of cells (n=3). (**D**) Transmission electron microscopy was used to observe the changes in the mitochondrial ultrastructure of each group of cells (scale bars: 2 μm and 500 nm). (**E** and **F**) Immunofluorescence staining of SOX9, Col II, and MMP13 in each group of cells (scale bar: 50 μm). (**G**) Average fluorescence intensity (n=3). (**H**) Determination of Fe^{2+} content (n=10). (**I**–**K**) RT-qPCR was used to detect the mRNA expression levels of p53, SLC7A11, and GPX4 (n=10). **P < 0.01, ***P < 0.001. The red arrow indicates the mitochondrial morphology. All data were from at least three repeated experiments, and each repeated experiment was independently detected three times.

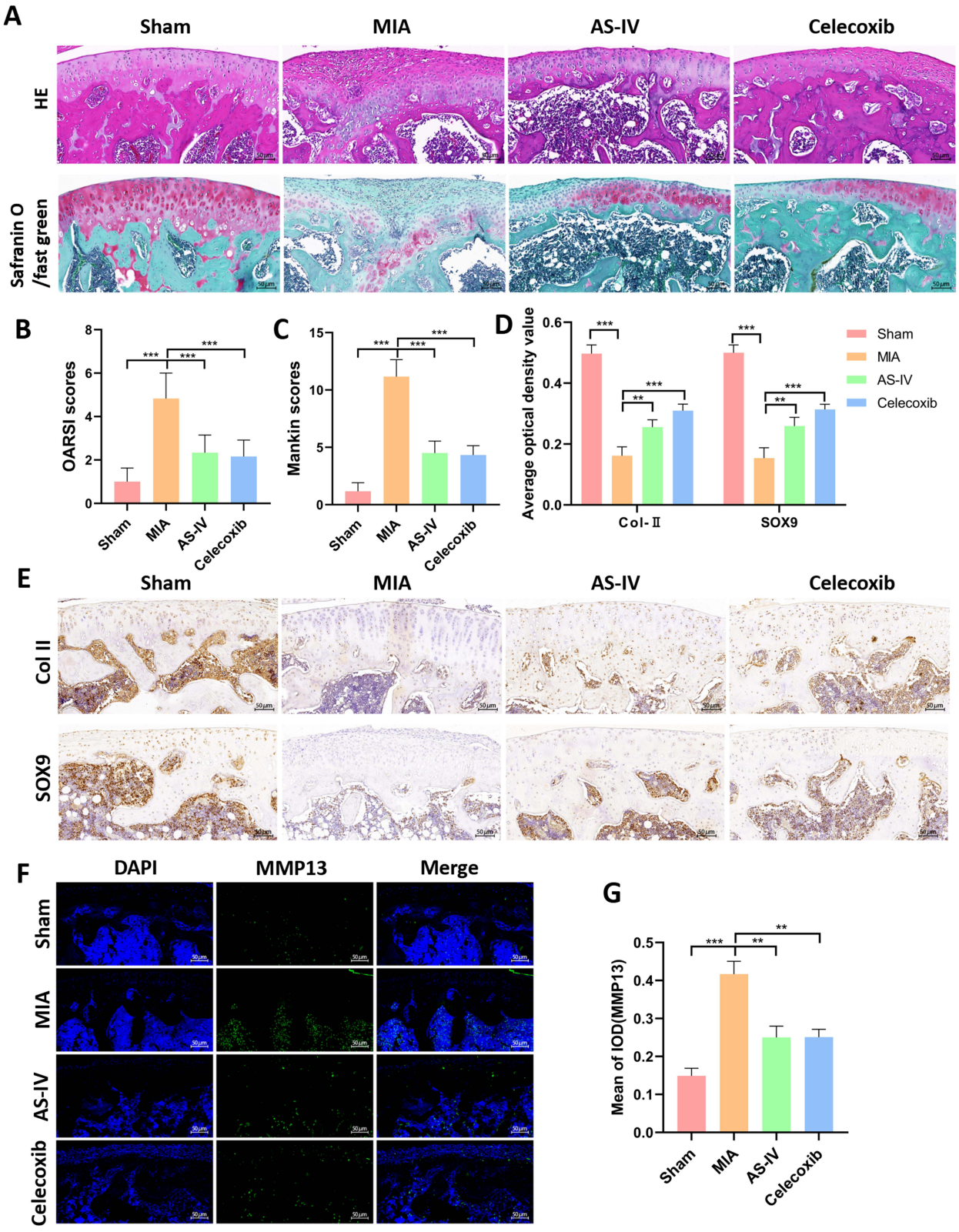

Figure 5 AS-IV can improve cartilage damage and inhibit matrix degradation in OA rats. (**A**) HE staining and Safranin O/Fast Green staining were used to evaluate the degree of cartilage damage (scale bar: 50 μm). (**B** and **C**) OARSI score and Mankin score. (**D** and **E**) Immunohistochemical staining was used to detect the expression of Col II and SOX9 proteins in cartilage tissues (scale bar: 50 μm). (**F**) Immunofluorescence staining was used to detect the expression of MMP13 in cartilage tissues (scale bar: 50 μm). (**G**) The average optical density value of MMP13 (n = 3). **P < 0.01, ***P < 0.001.

https://doi.org/10.2147/JIR.S572167

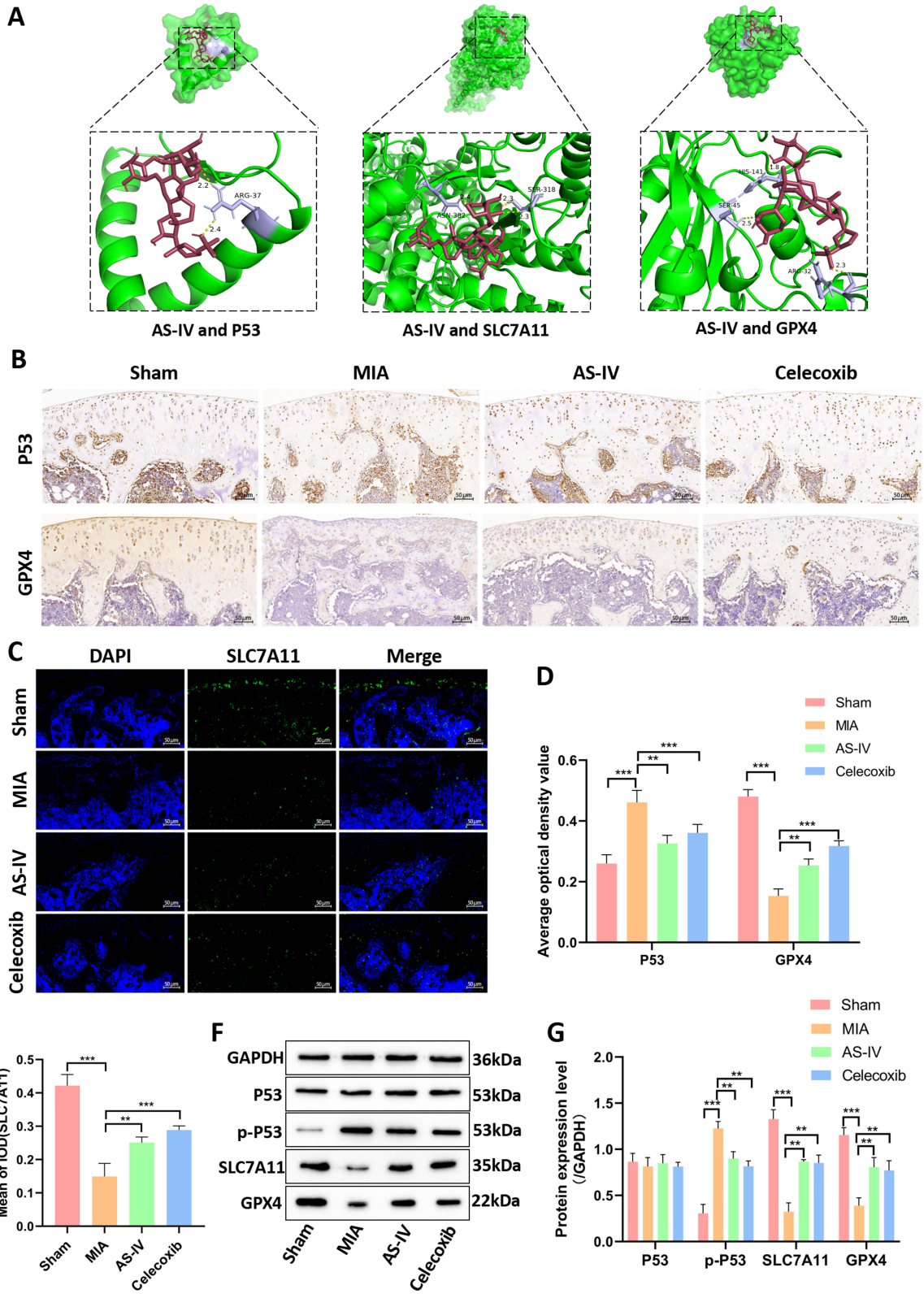

Figure 6 AS-IV can regulate the p53/SLC7A11/GPX4 pathway in cartilage tissue. (**A**) Visualization of molecular docking results: AS-IV with p53, AS-IV with SLC7A11, and AS-IV with GPX4. (**B**–**E**) Immunofluorescence and immunohistochemical staining were used to detect the expression of p53, SLC7A11, and GPX4 in cartilage tissue (n = 3, scale bar: 50 μm). (**F**) Protein electrophoresis image. (**G**) Protein expression levels of p53, p-p53, SLC7A11, and GPX4 in each group (n = 3). **P < 0.01, ***P < 0.001. All data were from at least three repeated experiments, and each repeated experiment was independently detected three times.

immunofluorescence staining, and Western blotting. The results showed that after AS-IV treatment, the expression of p53 in cartilage tissue was significantly decreased, while the expression of SLC7A11 and GPX4 was increased, which was comparable to the intervention effect of Celecoxib (Figure 6B–G). The above results indicate that AS-IV can regulate the p53/SLC7A11/GPX4 pathway in cartilage tissue.

AS-IV Can Inhibit Ferroptosis and Lipid Peroxidation in Cartilage Tissue

The ROS levels in cartilage tissues of each group were detected by flow cytometry. Compared with the Sham group, the ROS levels in the MIA group were significantly increased. After AS-IV treatment, the ROS levels were significantly decreased ($P < 0.01$, Figure 7A and B). The ultrastructure of mitochondria in cartilage tissues was observed by transmission electron microscopy. Compared with the MIA group, the mitochondrial morphology, membrane integrity, and cristae arrangement in the AS-IV group were all restored (Figure 7C), which was consistent with the effect of the Celecoxib group. Meanwhile, after AS-IV treatment, the Fe^{2+} content in cartilage tissues was significantly decreased ($P < 0.01$, Figure 7D), the GSH level was significantly

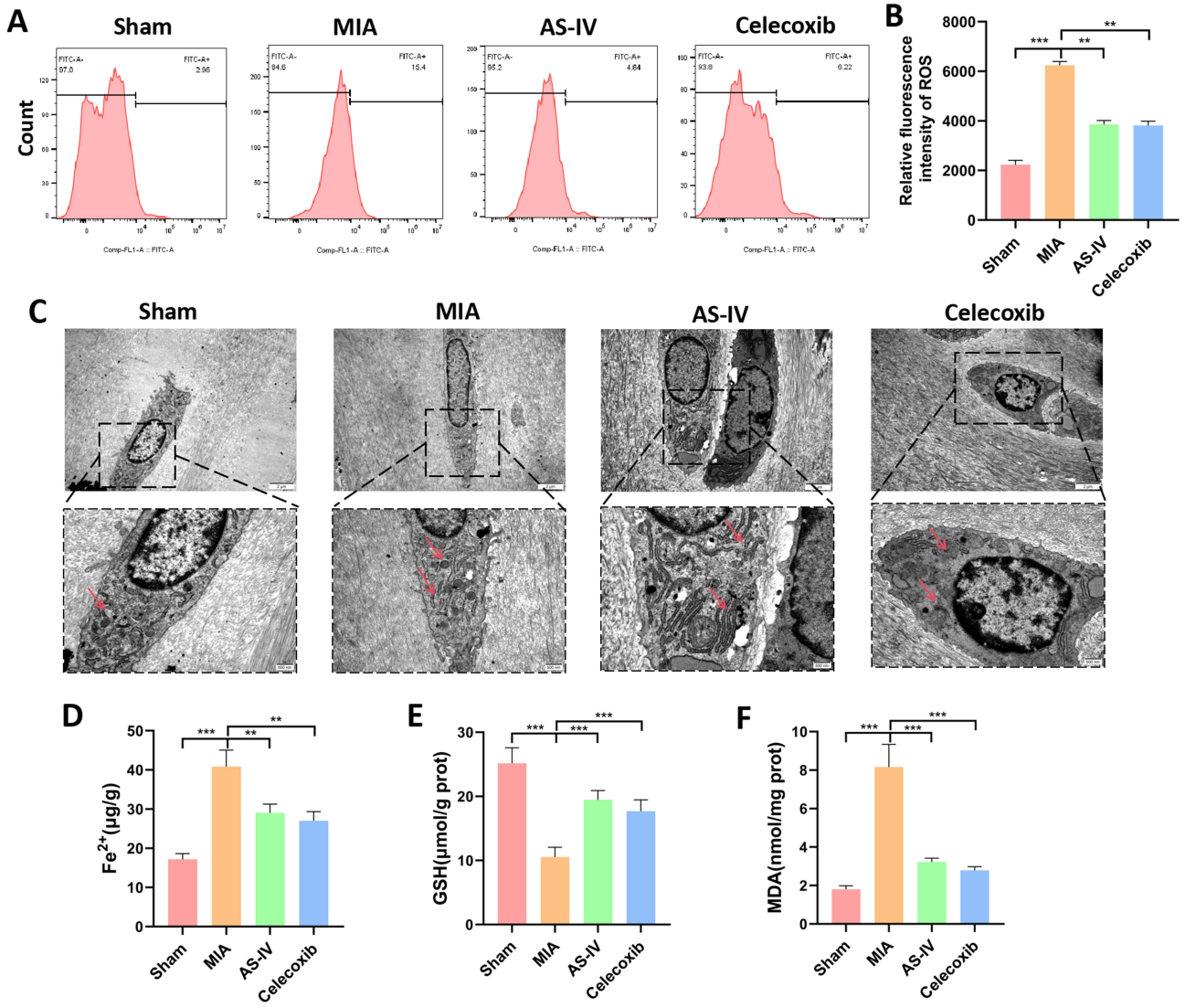

Figure 7 AS-IV can inhibit ferroptosis and lipid peroxidation in cartilage tissue. (**A** and **B**) Flow cytometry was used to detect the ROS levels in cartilage tissue (n = 3). (**C**) Transmission electron microscopy was used to observe the changes in mitochondrial ultrastructure in each group (scale bars: 2 μm and 500 nm). (**D**) The Fe2+ content in cartilage tissue (n = 10). (**E** and **F**) Determination of GSH and MDA contents in cartilage tissue (n = 10). **P < 0.01, ***P < 0.001. The red arrow indicates the mitochondrial morphology. All data were from at least three repeated experiments, and each repeated experiment was independently detected three times.

https://doi.org/10.2147/JIR.S572167

increased ($P < 0.01$, Figure 7E), and the MDA level was significantly decreased ($P < 0.01$, Figure 7F). In conclusion, AS-IV can inhibit ferroptosis and lipid peroxidation in cartilage tissues and has a certain protective effect on cartilage tissues.

Discussion

OA is a chronic joint disease that seriously affects the quality of life of patients. Its main features are the damage and degeneration of articular cartilage. Although there are currently various treatment methods, they mainly focus on symptom relief, and there is a lack of targeted treatment means to effectively block the progression of the disease. This study focuses on the efficacy and mechanism of action of AS-IV in the treatment of OA. First, it clarifies the key role of chondrocyte ferroptosis in the progression of OA, as well as the specific mechanism by which AS-IV inhibits chondrocyte ferroptosis through the regulation of the p53/SLC7A11/GPX4 axis. In in -vitro experiments, the IL-1β-induced chondrocyte ferroptosis model shows that overexpression of p53 exacerbates this process, while AS-IV can effectively improve the ferroptosis state of cells. In the in-vivo OA rat model, AS-IV significantly reduces the degree of cartilage damage and lowers the OARSI score and Mankin score. These research results indicate that AS-IV has the potential to treat OA, which is closely related to the inhibition of chondrocyte ferroptosis.

As the only cell type in articular cartilage, chondrocytes play a dual role in the pathological process of OA. They are not only the maintainers of ECM homeostasis but also the core drivers of the pathological cascade reaction.[26,27] In this in vitro study, the SW1353 cell model treated with IL-1β was used as the research object. The results showed that after IL-1β induction, chondrocytes exhibited mitochondrial atrophy, increased intracellular ROS, depletion of GSH and GPX4, and accumulation of Fe^{2+} and MDA. These results were consistent with previous studies, indicating that IL-1β can induce chondrocytes to enter the ferroptosis state.[28] Some studies have found that the expression of GPX4 in the cartilage of OA model rats decreased,[29] further confirming that ferroptosis is involved in the development of OA. In terms of ECM degradation, previous literature has shown that IL-1β can promote the degradation of chondrocyte ECM and aggravate cell damage.[30] In this study, it was found that IL-1β can increase the level of MMP13 and decrease the levels of Col II and SOX9, which is consistent with the results of previous literature. Therefore, there is sufficient evidence to use IL-1β to induce the OA cell model.

Ferroptosis is an iron-dependent form of cell death driven by lipid peroxidation and is considered an important mechanism of chondrocyte apoptosis in OA.[31] As a transcription factor, p53 is involved in regulating the osteogenesis-osteoclastogenesis balance and oxidative stress, and can regulate the expression of genes related to ferroptosis, including SLC7A11 and GPX4.[32] Meanwhile, previous studies have found that the expression of p53 is closely related to the severity of patients with knee osteoarthritis.[33] The results of this study showed that the degree of ferroptosis was aggravated in the state of p53 overexpression. SLC7A11 is a cystine-glutamate antiporter responsible for transporting cystine into cells and then synthesizing GSH.[34] Previous studies have found that miR-19b-3p can aggravate ferroptosis and damage of OA cartilage by inhibiting SLC7A11.[35] As a key antioxidant defense molecule, GPX4 can scavenge peroxides in mitochondria, prevent mitochondrial DNA damage and respiratory chain dysfunction, and maintain cellular energy metabolism.[36] Downregulation of GPX4 can increase the sensitivity of chondrocytes to oxidative stress and aggravate ECM degradation through the MAPK/NF-κB pathway.[37] Meanwhile, ferroptosis triggered by ROS leads to the release of iron ions in cells, and free iron ions will generate more ROS through the Fenton reaction, continuously exacerbating cell damage and death.[38] A large number of studies have confirmed that p53 can inhibit the expression of SLC7A11 and GPX4, thereby reducing the uptake of cystine and the synthesis of GSH in cells, triggering mitochondrial dysfunction, leading to the accumulation of lipid peroxidation, and inducing ferroptosis.[39] In in vitro cell experiments, the ferroptosis inhibitor Fer-1 was used as a positive control drug. The results showed that after treatment with AS-IV, the expression of p53 in cells was significantly decreased, while the expression of SLC7A11 and GPX4 was upregulated, the level of GSH was increased, and the levels of ROS and MDA were decreased, thereby inhibiting ferroptosis, which was comparable to the effect of Fer-1. To further verify the target of AS-IV, a rescue experiment was conducted, and it was found that overexpression of p53 could weaken the intervention effect of AS-IV on chondrocytes. These results suggest that AS-IV inhibits ferroptosis of chondrocytes by mediating the p53/SLC7A11/GPX4 axis and protects chondrocytes from oxidative stress and inflammatory damage.

The main pathological feature of OA is that the degradation of ECM exceeds its synthesis, leading to a decrease in the net content of cartilage matrix. The cartilage covering the articular bone surface may even be completely depleted.[40] Due to the reduced synthesis of chondrocytes and the activation of enzymes that degrade the cartilage matrix, there is a loss of aggrecan in OA, ultimately causing cartilage damage.[41] The results of this study found that AS-IV can reduce the level of MMP13 in chondrocytes and increase the levels of Col II and SOX9. Some studies have found that the content of MMP13 in the cartilage tissue of OA patients is significantly higher than that in normal people.[42] MMP13 is a cartilage matrix-degrading enzyme that can degrade cartilage ECM, leading to damage to the structure and function of cartilage and accelerating cartilage degeneration.[43] SOX9 is a chondrogenic gene that participates in regulating the differentiation of chondrocytes, promotes the synthesis of ECM components such as Col II and proteoglycans by chondrocytes, and maintains the normal phenotype and function of chondrocytes.[44] Col II is the main component of the extracellular matrix of articular cartilage. After a large amount of Col II is degraded by degrading enzymes such as MMP13, the mechanical properties of cartilage decrease, and its elasticity and toughness deteriorate, further aggravating the condition of OA.[45] The results of this study indicate that AS-IV can inhibit the degradation of chondrocyte ECM and reduce the degree of cell damage.

To further clarify the protective effect of AS-IV on cartilage, an in vivo experiment was carried out by establishing an OA rat model using the MIA method. Methods such as HE, Safranin O/Fast Green staining, immunofluorescence, and immunohistochemical staining were used to detect cartilage damage. Compared with the MIA group, AS-IV improved the pathological changes of cartilage tissue and reduced the OARSI and Mankin scores. The OARSI and Mankin scores are commonly used pathological scoring criteria for OA, reflecting the integrity of the cartilage surface and the degree of cartilage matrix degeneration, respectively.[46] The results of molecular docking showed that AS-IV had a good binding effect with p53, SLC7A11, and GPX4. Meanwhile, after AS-IV intervention, the levels of p53, ROS, MDA, and Fe^{2+} in the cartilage tissue of OA rats decreased, while the levels of GSH, SLC7A11, and GPX4 increased, and the degree of ECM degradation was alleviated. The results of the in vivo experiment were basically consistent with those of the cell experiment, which more clearly indicated that AS-IV could mediate the p53/SLC7A11/GPX4 axis, improve lipid peroxidation and ferroptosis of chondrocytes, regulate ECM degradation, and alleviate cartilage damage.

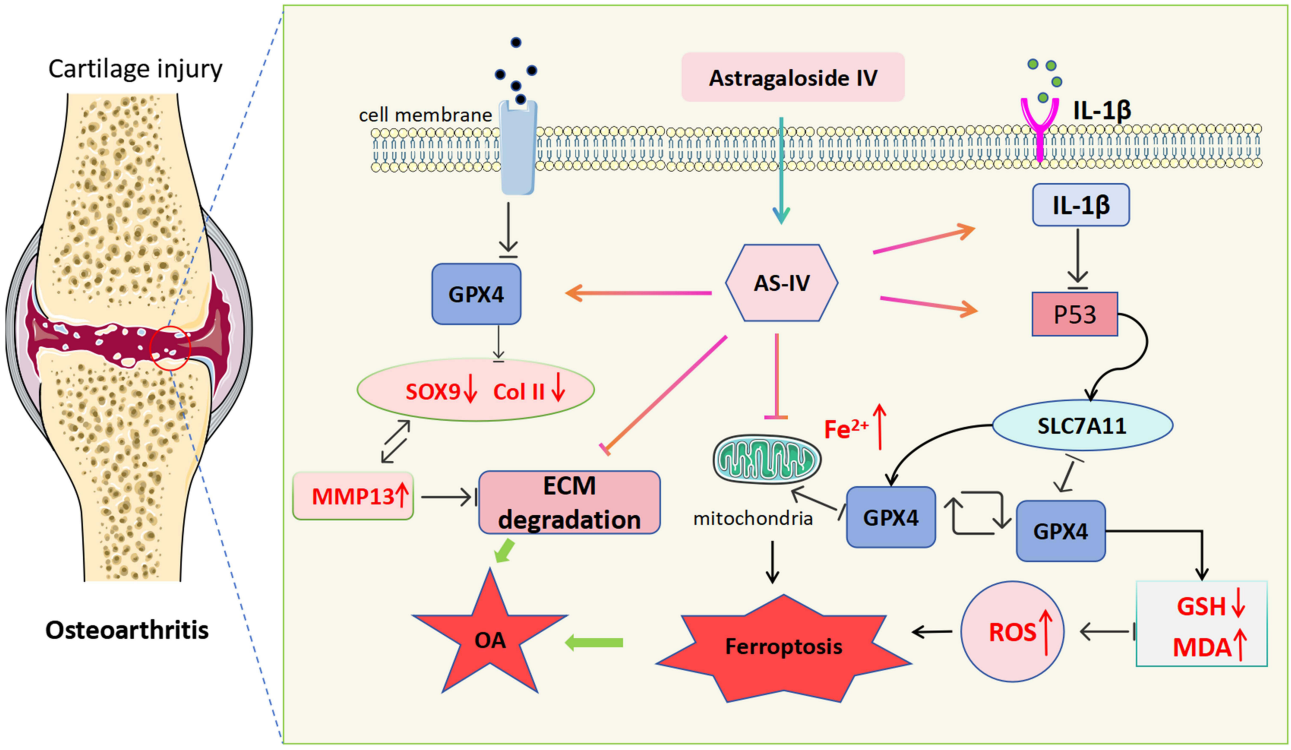

Figure 8 Schematic diagram of the mechanism by which AS-IV inhibits ferroptosis of chondrocytes through the p53/SLC7A11/GPX4 axis and improves OA cartilage injury.

https://doi.org/10.2147/JIR.S572167

In conclusion, this study systematically confirmed through in vitro and in vivo experiments that AS-IV has significant efficacy in the treatment of OA. Its mechanism of action includes mediating the p53/SLC7A11/GPX4 axis to inhibit ferroptosis of chondrocytes, regulating ECM degradation, and exerting antioxidant effects. This study provides new ideas and theoretical basis for the treatment of OA and has important clinical application prospects. Although this study has made important progress, there are still some limitations. First of all, this study mainly focused on experiments in vitro and in animal models. In the future, the therapeutic effect of AS-IV needs to be further verified in clinical trials.

Conclusion

Through systematic exploration and verification, this study confirmed that AS-IV inhibits ferroptosis and lipid peroxidation of chondrocytes by mediating the p53/SLC7A11/GPX4 axis, regulates ECM degradation, and improves cartilage damage, thereby alleviating OA (Figure 8). This finding provides strong evidence for the development of AS-IV as a potential therapeutic drug. In subsequent studies, intervention experiments of AS-IV on human primary chondrocytes, as well as pharmacokinetic and safety studies of AS-IV will be carried out.

Abbreviations

AS-IV, Astragaloside IV; MIA, monosodium iodoacetate; OA, osteoarthritis; ECM, extracellular matrix; GSH, glutathione; MDA, malondialdehyde; ROS, reactive oxygen species; SOX9, SRY - box transcription factor 9; Col II, type II collagen; MMP13, matrix metalloproteinase 13; OARSI, osteoarthritis research society international; Fer-1, ferrostatin-1; IL-1β, interleukin-1 beta; TEM, transmission electron microscopy; RT-qPCR, reverse transcription quantitative polymerase chain reaction; CKK-8, cell counting kit-8.

Data Sharing Statement

The data can be provided by the corresponding author upon request.

Ethical Approval

All animal experiments were approved by the Experimental Animal Ethics Committee of the First Affiliated Hospital of Anhui University of Chinese Medicine (AZYFY-2025-1017).

Author Contributions

ZFT: Writing-Original Draft; Methodology; Investigation. LLC: Visualization; Software; Data Curation. ML: Visualization; Software; Writing-Review & Editing. JJC: Validation; Data Curation; Writing-Review & Editing. CBH: Writing-Review & Editing; Project administration; Conceptualization; Resources. All authors took part in drafting, revising, or critically reviewing the article; gave final approval of the version to be published; have agreed on the journal to which the article has been submitted; and agree to be accountable for all aspects of the work.

Funding

This study was supported by the National Natural Science Foundation of China (No.82104782), Clinical Medical Research Transformation Special Project of Anhui Province (No.202304295107020114 and No.202304295107020115), and Xin ‘an Institute of Medicine and Traditional Chinese Medicine Modernization (No.2023CXMMTCM004 and No.2023CXMMTCM015).

Disclosure

The authors report no conflicts of interest in this work.

References

1. Salman LA, Ahmed G, Dakin SG, Kendrick B, Price A. Osteoarthritis: a narrative review of molecular approaches to disease management. *Arthritis Res Ther*. 2023;25(1):27. doi:10.1186/s13075-023-03006-w
2. Yunus MHM, Nordin A, Kamal H. Pathophysiological perspective of osteoarthritis. *Medicina*. 2020;56(11). doi:10.3390/medicina56110614

3. Tuncay Duruöz M, Öz N, Gürsoy DE, Hande Gezer H. Clinical aspects and outcomes in osteoarthritis. *Best Pract Res Clin Rheumatol*. 2023;37(2):101855. doi:10.1016/j.berh.2023.101855
4. Allen KD, Thoma LM, Golightly YM. Epidemiology of osteoarthritis. *Osteoarthritis Cartilage*. 2022;30(2):184–195. doi:10.1016/j.joca.2021.04.020
5. Kolasinski SL, Neogi T, Hochberg MC, et al. 2019 American college of rheumatology/arthritis foundation guideline for the management of osteoarthritis of the hand, hip, and knee. *Arthritis Care Res*. 2020;72(2):149–162. doi:10.1002/acr.24131
6. Kong H, Han JJ, Dmitrii G, Zhang XA. Phytochemicals against osteoarthritis by inhibiting apoptosis. *Molecules*. 2024;29(7):1487. doi:10.3390/molecules29071487
7. Zhang S, Zhan J, Li M, et al. Therapeutic potential of traditional chinese medicine against osteoarthritis: targeting the wnt signaling pathway. *Am J Chin Med*. 2024;52(7):2021–2052. doi:10.1142/s0192415x24500782
8. Liu YX, Song XM, Dan LW, et al. Astragali Radix: comprehensive review of its botany, phytochemistry, pharmacology and clinical application. *Arch Pharm Res*. 2024;47(3):165–218. doi:10.1007/s12272-024-01489-y
9. Chen K, Yu Y, Wang Y, et al. Systematic pharmacology and experimental validation to reveal the alleviation of astragalus membranaceus regulating ferroptosis in osteoarthritis. *Drug Des Devel Ther*. 2024;18:259–275. doi:10.2147/dddt.S441350
10. Liang Y, Chen B, Liang D, et al. Pharmacological effects of astragaloside IV: a review. *Molecules*. 2023;28(16):6118. doi:10.3390/molecules28166118
11. Yang K, Xie Q, Tang T, et al. Astragaloside IV as a novel CXCR4 antagonist alleviates osteoarthritis in the knee of monosodium iodoacetate-induced rats. *Phytomedicine*. 2023;108:154506. doi:10.1016/j.phymed.2022.154506
12. Xu H, Jing-Bo W, Chen YP, Huang W, Wei ZB. Astragaloside IV protects against IL-1β-induced chondrocyte damage via activating autophagy. *Curr Mol Med*. 2024;24(11):1382–1389. doi:10.2174/0115665240249154231016080115
13. Wang L, Liu C, Wang L, Tang B. Astragaloside IV mitigates cerebral ischaemia-reperfusion injury via inhibition of P62/Keap1/Nrf2 pathway-mediated ferroptosis. *Eur J Pharmacol*. 2023;944:175516. doi:10.1016/j.ejphar.2023.175516
14. Iantomasi T, Aurilia C, Donati S, et al. Oxidative stress, MicroRNAs, and long non-coding RNAs in osteoarthritis pathogenesis: cross-talk and molecular mechanisms involved. *Int J Mol Sci*. 2025;26(13):6428. doi:10.3390/ijms26136428
15. Liu S, Pan Y, Li T, et al. The role of regulated programmed cell death in osteoarthritis: from pathogenesis to therapy. *Int J Mol Sci*. 2023;24(6):5364. doi:10.3390/ijms24065364
16. Wu B, Luo Z, Chen Z, et al. Paeoniflorin mitigates iron overload-induced osteoarthritis by suppressing chondrocyte ferroptosis via the p53/SLC7A11/GPX4 pathway. *Int Immunopharmacol*. 2025;162:115111. doi:10.1016/j.intimp.2025.115111
17. Gong Z, Wang Y, Li L, Li X, Qiu B, Hu Y. Cardamonin alleviates chondrocytes inflammation and cartilage degradation of osteoarthritis by inhibiting ferroptosis via p53 pathway. *Food Chem Toxicol*. 2023;174:113644. doi:10.1016/j.fct.2023.113644
18. He R, Wei Y, Peng Z, et al. α-Ketoglutarate alleviates osteoarthritis by inhibiting ferroptosis via the ETV4/SLC7A11/GPX4 signaling pathway. *Cell Mol Biol Lett*. 2024;29(1):88. doi:10.1186/s11658-024-00605-6
19. Xiao J, Luo C, Li A, et al. Icariin inhibits chondrocyte ferroptosis and alleviates osteoarthritis by enhancing the SLC7A11/GPX4 signaling. *Int Immunopharmacol*. 2024;133:112010. doi:10.1016/j.intimp.2024.112010
20. Shaban NS, Radi AM, Abdelgawad MA, et al. Targeting some key metalloproteinases by nano-naringenin and amphora coffeaeformis as a novel strategy for treatment of osteoarthritis in rats. *Pharmaceuticals*. 2023;16(2):260. doi:10.3390/ph16020260
21. Runz M, Rusche D, Schmidt S, Weihrauch MR, Hesser J, Weis CA. Normalization of HE-stained histological images using cycle consistent generative adversarial networks. *Diagn Pathol*. 2021;16(1):71. doi:10.1186/s13000-021-01126-y
22. Zhang H, Jiang H, Wei Q, et al. Suppression of inflammation by Si Miao San in experimental rheumatoid arthritis through modulation of the AKT/ROS/autophagy axis. *J Inflamm Res*. 2025;18:9459–9476. doi:10.2147/jir.S524871
23. Xu M, Chen X, Du S, Xu H, Liu C. Isoginkgetin protects chondrocytes and inhibits osteoarthritis through NF-κB and P21 signaling pathway. *Mol Med*. 2025;31(1):246. doi:10.1186/s10020-025-01302-6
24. Zhuang C, Li E, Li WK, et al. Modified qianghuo shengshi decoction ameliorates osteoarthritis via inhibiting PI3K/Akt pathway-related ferroptosis. *J Cell Mol Med*. 2025;29(13):e70691. doi:10.1111/jcmm.70691
25. Kim MJ, Yang YJ, Heo JW, et al. Potential chondroprotective effect of Artemisia annua L. Water extract on SW1353 cell. *Int J Mol Sci*. 2025;26(5):1901. doi:10.3390/ijms26051901
26. Adam MS, Zhuang H, Ren X, Zhang Y, Zhou P. The metabolic characteristics and changes of chondrocytes in vivo and in vitro in osteoarthritis. *Front Endocrinol*. 2024;15:1393550. doi:10.3389/fendo.2024.1393550
27. Cao S, Wei Y, Xu H, et al. Crosstalk between ferroptosis and chondrocytes in osteoarthritis: a systematic review of in vivo and in vitro studies. *Front Immunol*. 2023;14:1202436. doi:10.3389/fimmu.2023.1202436
28. Chen BY, Pathak JL, Lin HY, et al. Inflammation Triggers Chondrocyte Ferroptosis in TMJOA via HIF-1α/TFRC. *J Dent Res*. 2024;103(7):712–722. doi:10.1177/00220345241242389
29. Ruan Q, Wang C, Zhang Y, Sun J. Ruscogenin attenuates cartilage destruction in osteoarthritis through suppressing chondrocyte ferroptosis via Nrf2/SLC7A11/GPX4 signaling pathway. *Chem Biol Interact*. 2024;388:110835. doi:10.1016/j.cbi.2023.110835
30. Liang C, Xing H, Wang C, Xu X, Hao Y, Qiu B. Resveratrol protection against IL-1β-induced chondrocyte damage via the SIRT1/FOXO1 signaling pathway. *J Orthop Surg Res*. 2022;17(1):406. doi:10.1186/s13018-022-03306-y
31. Yao X, Sun K, Yu S, et al. Chondrocyte ferroptosis contribute to the progression of osteoarthritis. *J Orthop Translat*. 2021;27:33–43. doi:10.1016/j.jot.2020.09.006
32. Zhao C, Kong K, Liu P, et al. Regulating obesity-induced osteoarthritis by targeting p53-FOXO3, osteoclast ferroptosis, and mesenchymal stem cell adipogenesis. *Nat Commun*. 2025;16(1):4532. doi:10.1038/s41467-025-59883-z
33. Zhang X, Shi K, Ruan A, Chen P, Zhang T, Wang Q. Expression characteristics of miR-502-5p/p53/NF-κB signaling pathway in patients with different degrees of knee osteoarthritis: a cross-sectional observational study with methodological limitations. *J Orthop Surg Res*. 2025;20(1):781. doi:10.1186/s13018-025-06134-y
34. Wang Z, Wang Y, Shen N, et al. AMPKα1-mediated ZDHHC8 phosphorylation promotes the palmitoylation of SLC7A11 to facilitate ferroptosis resistance in glioblastoma. *Cancer Lett*. 2024;584:216619. doi:10.1016/j.canlet.2024.216619
35. Kong R, Ji L, Pang Y, Zhao D, Gao J. Exosomes from osteoarthritic fibroblast-like synoviocytes promote cartilage ferroptosis and damage via delivering microRNA-19b-3p to target SLC7A11 in osteoarthritis. *Front Immunol*. 2023;14:1181156. doi:10.3389/fimmu.2023.1181156

36. Xue Q, Yan D, Chen X, et al. Copper-dependent autophagic degradation of GPX4 drives ferroptosis. *Autophagy*. 2023;19(7):1982–1996. doi:10.1080/15548627.2023.2165323
37. Miao Y, Chen Y, Xue F, et al. Contribution of ferroptosis and GPX4's dual functions to osteoarthritis progression. *EBioMedicine*. 2022;76:103847. doi:10.1016/j.ebiom.2022.103847
38. Li T, Wang N, Yi D, et al. ROS-mediated ferroptosis and pyroptosis in cardiomyocytes: an update. *Life Sci*. 2025;370:123565. doi:10.1016/j.lfs.2025.123565
39. Lei M, Zhang YL, Huang FY, et al. Gankyrin inhibits ferroptosis through the p53/SLC7A11/GPX4 axis in triple-negative breast cancer cells. *Sci Rep*. 2023;13(1):21916. doi:10.1038/s41598-023-49136-8
40. He Q, Lin Y, Chen B, et al. Vitamin K2 ameliorates osteoarthritis by suppressing ferroptosis and extracellular matrix degradation through activation GPX4's dual functions. *Biomed Pharmacother*. 2024;175:116697. doi:10.1016/j.biopha.2024.116697
41. Ruan H, Zhu T, Wang T, Guo Y, Liu Y, Zheng J. Quercetin modulates ferroptosis via the SIRT1/Nrf-2/HO-1 pathway and attenuates cartilage destruction in an osteoarthritis rat model. *Int J Mol Sci*. 2024;25(13):7461. doi:10.3390/ijms25137461
42. Wan Y, Li W, Liao Z, Yan M, Chen X, Tang Z. Selective MMP-13 inhibitors: promising agents for the therapy of osteoarthritis. *Curr Med Chem*. 2020;27(22):3753–3769. doi:10.2174/0929867326666181217153118
43. Staebler S, Lichtblau A, Gurbiel S, et al. MIA/CD-RAP regulates MMP13 and is a potential new disease-modifying target for osteoarthritis therapy. *Cells*. 2023;12(2):229. doi:10.3390/cells12020229
44. Mei Z, Yilamu K, Ni W, et al. Chondrocyte fatty acid oxidation drives osteoarthritis via SOX9 degradation and epigenetic regulation. *Nat Commun*. 2025;16(1):4892. doi:10.1038/s41467-025-60037-4
45. Sohn HS, Choi JW, Jhun J, et al. Tolerogenic nanoparticles induce type II collagen-specific regulatory T cells and ameliorate osteoarthritis. *Sci Adv*. 2022;8(47):eabo5284. doi:10.1126/sciadv.abo5284
46. Jin Z, Chang B, Wei Y, et al. Curcumin exerts chondroprotective effects against osteoarthritis by promoting AMPK/PINK1/Parkin-mediated mitophagy. *Biomed Pharmacother*. 2022;151:113092. doi:10.1016/j.biopha.2022.113092